Chinese Journal of Oceanology and Limnology
Vol. 29 No. 6, P. 1224-1236, 2011
DOI: 10.1007/s00343-011-0308-z

Meridional distribution of ^{226}Ra in the west Pacific and the Southern Ocean surface waters*

CHEN Zhigang (陈志刚)[1], HUANG Yipu (黄奕普)[1, **], CHEN Min (陈敏)[1], CAI Pinghe (蔡平河)[1], XING Na (邢娜)[1], CAI Yihua (蔡毅华)[1], CHEN Jinfang (陈锦芳)[1, 2]

[1] *College of Oceanography and Environment, Xiamen University, Xiamen 361005, China*

[2] *Bio-engineering College of Jimei University, Xiamen 361021, China*

Received Dec. 12, 2010; accepted in principle Feb. 24, 2011; accepted for publication Mar. 25, 2011

Abstract During the 13th (1996–1997) and the 19th (2002–2003) Chinese National Antarctica Research Expeditions, we collected 60 discrete surface seawater samples along the cruise from the Chanjiang River (Yangtze) estuary (30°59′S, 122°26′E) through Taiwan Strait, the South China Sea, and the Eastern Indian Ocean to Prydz Bay, Antarctica (69°10′S, 74°30′E), and analyzed them for the ^{226}Ra specific activity. The ^{226}Ra specific activity of the Chanjiang River estuary surface water (3.15 Bq/m^3) was found to be the highest among all the surface samples because of the desorption of ^{226}Ra from riverine particles. Between Chanjiang River estuary and 40°S, ^{226}Ra specific activity was found to be relatively uniform with a mean value of 1.07 Bq/m^3 (n=19, SD=0.14), similar to that of the open ocean. From 40°S to 65°S, ^{226}Ra specific activity increased intensively, then decreased moderately further southwards. Near the Antarctic shore, it increased again, to 2.31 Bq/m^3. This distribution was controlled by a combination of deep water upwelling, Southern Ocean fronts, water mixing and the continental ^{226}Ra import. In Prydz Bay and the adjacent sea area, the mean ^{226}Ra activity value was 2.26 Bq/m^3 (n=31, SD=0.28), with a relatively higher value outside of the bay and low ^{226}Ra activity value in the center of the bay. This was consistent with the topography and hydrological setting of the bay. In addition, we extended the study area northward to the Arctic, by combining the published ^{226}Ra dataset for surface water from the Bering Sea to the Japan Sea. We also discuss the ^{226}Ra distribution of high latitude oceanic surface water and its mechanisms.

Keyword: ^{226}Ra; Chanjiang River estuary; Antarctic; Prydz Bay; Leeuwin Current

1 INTRODUCTION

During the 13th and the 19th Chinese National Antarctica Research Expeditions (CHINARE), along the cruises from Chanjiang (Yangtze) River estuary (30°59′S, 122°26′E) through Taiwan Strait, the Java Sea, the Eastern Indian Ocean to Prydz Bay, Antarctica (69°10′S, 74°30′E) (spanning nearly 100 latitude degrees) we collected 60 surface seawater samples for ^{226}Ra measurement. Combining the ^{226}Ra data of surface seawater from the Bering Sea to the Japan Sea published by our laboratory, we depict a continuous and complete ^{226}Ra distribution for the surface sea water along a transect from the Bering Sea, through eastern Eurasian coastal waters to Antarctic coastal waters. We also discuss the ^{226}Ra distribution feature of high latitude ocean surface seawater and its mechanism.

^{226}Ra has a half-life of 1 600 years and has been regarded as the most important isotope after radiocarbon for investigating the rates of deep ocean circulation and mixing (Chung and Craig, 1980). Koczy (1958) first used ^{226}Ra to derive the vertical eddy diffusivities and the vertical water velocity in the deep sea. To date, the most vast and complete ^{226}Ra study of world oceans has been the GEOSECS Program (1967–1980) (Broecker et al., 1976; Chung and Craig, 1980; Chung, 1987; Ku et al., 1980). A primary aim of the program was to obtain detailed ^{226}Ra profiles of the oceans and, combining with other radioactive isotopes, to trace large scale mixing

* Supported by the National Natural Science Foundation of China (Nos. 40706033 and 40806031) and COMRA Program (Nos. DYXM-115-02-1-12 and DY115-01-2-5)

** Corresponding author: yphuang@xmu.edu.cn

and circulation of the ocean water (Chung, 1974; Chung and Craig, 1980).

In addition to bottom diffusion, continental input is another important source of ^{226}Ra to the ocean, making ^{226}Ra a useful tracer of the coastal marine processes (Moore, 2000). Therefore, since the GEOSECS program, most oceanic ^{226}Ra studies have been focused on the coastal area. ^{226}Ra has been successfully applied to trace coastal water mixing (Inoue et al., 2007; Moore, 2000), the residence time of the coastal water (Harada and Tsunogai, 1986; Lee et al., 2005; Nozaki et al., 1991), estuary processes (Key et al., 1985; Moore et al., 1995) and submarine groundwater discharge (Hussain et al., 1999; Hwang et al., 2005; Kim et al., 2005; Krest et al., 1999; Moore, 1996). In China, the isotopic oceanography group of the Xiamen University has laid the foundation of oceanic ^{226}Ra research, having done a great deal of oceanic ^{226}Ra studies in areas such the Jiulong River estuary (Shi et al., 1993; Xie et al., 1994a), the NE South China Sea (Huang et al., 1997; Xie et al., 1995), the Nansha sea area (Huang et al., 1996; Xie et al., 1996), the Arctic Ocean and the Bering Sea (Xing et al., 2003), the North Pacific Subtropical Gyre (Li et al., 2004; Yang et al., 2007) and the East China and Yellow Seas (Men et al., 2006; Men, 2008). Some other researchers in China have also investigated the geochemistry of ^{226}Ra in Prydz Bay, Antarctica and the East China Sea (Wu et al., 2001; Yin et al., 2004; Zhang et al., 2007; Zhang, 2007). There have also been lots of studies using ^{226}Ra to trace the coastal marine process of the eastern Eurasian continent marginal sea by foreign researchers (Harada and Tsunogai, 1986; Kim et al., 2005; Nozaki et al., 1989, 1991, 1998, 2001). Unfortunately, each study was restricted to a local sea area, and the results are different from each other.

During the GEOSECS program research, it was found that the ^{226}Ra specific activities of the Southern Ocean surface water were distinctly high (Ostlund et al., 1987). However, the ^{226}Ra sampling stations were sparse, and did not reach the Antarctic coastal waters. Chung and Applequist (1980) made a detailed ^{226}Ra study along a section from coastal waters to 58°S in the Weddell Sea, but their northernmost samples were still restricted to the south of the southern boundary of Antarctic Circumpolar Current. Wu et al. (2001) studied the ^{226}Ra distribution features of the surface seawater along the cruise running from the western Pacific, around the Southern Ocean to the eastern Indian Ocean. However, only a total of 16 samples were taken.

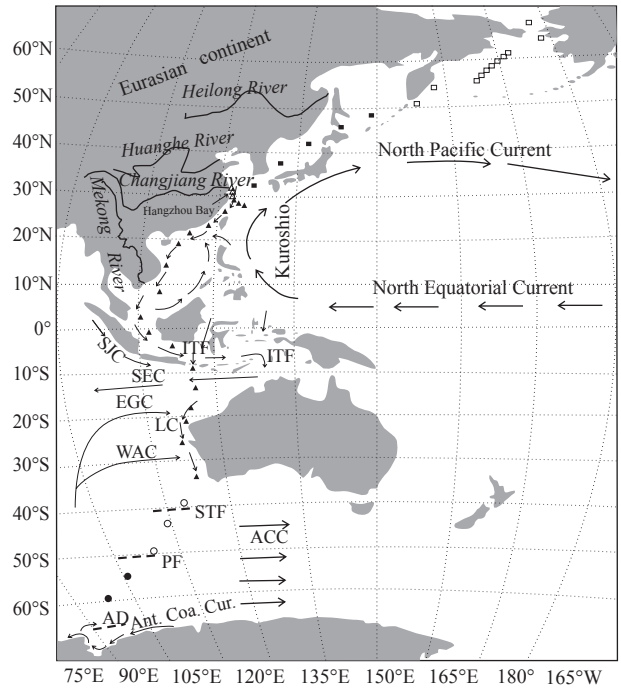

Fig.1 Locations of the sampling stations

ITF: Indonesian Throughflow; SJC: South Java Current; SEC: South Equatorial Current; EGC: subtropical Eastern Gyral Current; WAC: West Australian Current; LC: Leeuwin Current; ACC: Antarctic Circumpolar Current; STF: Subtropical Front; PF: Antarctic Polar Front ; AD: Antarctic Divergence.

Thus, a continuously and intensively sampled ^{226}Ra study that transects from subtropical seas to the Antarctic coastal waters is necessary.

2 METHOD

2.1 Sample collection

The sampling stations are shown in Fig.1. The samples from the Changjiang River estuary to 60°S were collected during the 13th CHINARE (from Nov. 1996 to Apr. 1997). Samples from Prydz Bay and its adjacent sea area were collected during both the 13th and the 19th CHINARE (from Nov. 2002 to Mar. 2003). Samples from the Bering Sea to the Japan Sea were sampled during the First Chinese National Arctic Research Expedition (from Jul. to Sept. 1999).

The water samples from Prydz Bay were collected by submerged pump while all the other samples were collected by small plastic kegs. Water samples in volumes of 100–120 L were collected and put into a plastic container. The seawater was then passed through a MnO_2-fiber (12 g) adsorption column, flowing from the column bottom to the column top. The flow speed was controlled at 200–250 cm^3/min

to ensure the quantitative adsorption of radium. The MnO_2 -fiber was taken out of the column after the enrichment process and water held in the fiber was squeezed out gently before it was sealed inside a plastic bag and taken back to the onshore laboratory for ^{226}Ra measurement. The procedure of MnO_2 -fiber preparation and in situ concentration of Ra from seawater had been discussed in detail by Xie et al. (1994b), and is similar to the pioneer method established by Moore and Reid (1973).

2.2 Measurement

The analyzer and method of this study was same as Yang et al. (2007). The ^{226}Ra specific activity was calculated by the Eq.1:

$$A = \frac{K\left(\frac{N_s}{t_s} - \frac{N_b}{t_b}\right)}{\alpha \cdot V \cdot \eta_c \cdot \eta_d} \quad (1)$$

where A is the specific activity of ^{226}Ra (Bq/m^3) in the water sample, K is the counting coefficient for ^{226}Ra (Bq/cpm), N_s and N_b are the total counts of sample and background respectively, and t_s and t_b (min) are the counting time of the sample and the background respectively, α is the ingrown coefficient of ^{222}Rn, V is the sample volume (m^3), η_c is the enriched efficiency of MnO_2-fiber for ^{226}Ra, η_d is the emanation efficiency of ^{222}Rn from MnO_2-fiber. α was calculated by the equation Eq.2:

$$\alpha = 1 - e^{-\lambda t} \quad (2)$$

where λ is the decay constant of ^{222}Rn, t is the time spent for ^{222}Rn growth and accumulation.

To assess the enrichment efficiency of MnO_2-fiber for ^{226}Ra (η_c), two columns, each containing 12 g MnO_2-fiber, were used in series to extract radium from seawater. The results showed that less than 1% of the total ^{226}Ra was retained in the second column, and the mean enrichment efficiency of MnO_2-fiber for ^{226}Ra was 99.2%±0.4%. The emanation efficiency of ^{222}Rn from MnO_2-fiber (η_d) was determined by adding a ^{226}Ra standard solution with a known activity onto the MnO_2-fiber directly. After ^{222}Rn accumulation, it was transferred into the detector cells for counting. The results showed that η_d was 91.0%±1.1%. The counting coefficient of ^{226}Ra (K) was determined by using ^{226}Ra standard solution sealed in the diffusion tube: after ^{222}Rn accumulation it was transferred to the detector cells for counting. The results show that the counting coefficient of ^{226}Ra (K) ranged from 7.10 to 9.30 mBq/cpm, with different values for different detector cells. In our experiment, the counting coefficient of ^{226}Ra was determined for each detector cell, and used for the calculation of ^{226}Ra specific activity for the given sample.

K can be calculated by the Eq.3:

$$K = \frac{A_s \cdot \alpha}{\left(\frac{N_s}{t_s} - \frac{N_b}{t_b}\right)} \quad (3)$$

where A_s is the activity of ^{226}Ra standard and other symbols are as for Eq.1.

All of the reported errors were propagated from one sigma counting uncertainty, which included contributions from the background counting, sample counting and the overall efficiency.

3 RESULT AND DISCUSSION

The ^{226}Ra activities of the surface seawater from Changjiang River estuary to 60°S are shown in Table 1. The ^{226}Ra activities of the surface seawater of Prydz Bay and its adjacent sea area are shown in Table 2. Fig.2 shows the meridional distribution of ^{226}Ra. For the stations south of 60°S, the data of the section III in Table 2 are used. Detailed ^{226}Ra distribution features of various sea areas are discussed below.

3.1 ^{226}Ra distribution in the surface seawater from the Changjiang River estuary and adjacent sea area

Station 40 was located at the outside of the Changjiang River estuary, while stations 39 and 38 were located at the outside of the Hangzhou Bay. The mean ^{226}Ra specific activity of these three samples was 2.78 Bq/m^3 (n=3, SD=0.32). Station 40 had the highest ^{226}Ra specific activity of 3.15 Bq/m^3, while ^{226}Ra specific activities of the station 39 and 38 were similar, being 2.62 and 2.57 Bq/m^3 respectively. The ^{226}Ra specific activities of these samples were obviously higher than those of their adjacent stations (Table 1 and Fig.2). Comparison of ^{226}Ra activities of the three samples clearly revealed that the Changjiang River water flows southward along the shore at the time of sampling.

Increased ^{226}Ra in the estuary mixing zone is a common phenomenon which can affect the river discharge flux of ^{226}Ra to the ocean and has attracted a lot of studies (Table 3). In river and ground waters radium strongly adsorbs to particles; in seawater it is primarily dissolved. These differences in chemical

Table 1 ^{226}Ra specific activity of surface seawater sampled in the cruise from the Changjiang River estuary to 60°S

Station	Latitude	Longitude	^{226}Ra (Bq/m^3)	Station	Latitude	Longitude	^{226}Ra (Bq/m^3)
16	59°45′S	83°42′E	2.28±0.04	29	3°31′N	105°38′E	1.06±0.03
17	55°13′S	90°38′E	2.04±0.04	30	8°38′N	109°16′E	1.04±0.03
18	49°57′S	98°02′E	2.06±0.04	31	14°15′N	109°39′E	1.10±0.03
19	44°32′S	104°02′E	1.64±0.04	32	19°10′N	113°05′E	1.14±0.03
20	39°46′S	108°31′E	0.85±0.03	1	22°02′N	114°34′E	1.38±0.04
21	34°24′S	113°24′E	1.26±0.04	33	23°19′N	118°08′E	0.87±0.03
22	27°37′S	112°55′E	1.05±0.03	34	26°23′N	121°48′E	1.03±0.03
23	21°00′S	113°27′E	1.16±0.03	35	27°59′N	125°03′E	1.02±0.03
24	17°54′S	114°03′E	1.14±0.03	36	28°26′N	124°22′E	0.87±0.03
25	13°50′S	114°53′E	1.06±0.03	37	28°55′N	123°53′E	1.26±0.03
26	8°41′S	115°46′E	1.03±0.03	38	29°58′N	122°36′E	2.57±0.04
27	4°39′S	111°36′E	1.11±0.03	39	30°17′N	122°37′E	2.62±0.08
28	0°43′S	107°13′E	0.88±0.03	40	30°59′N	122°26′E	3.15±0.08

behavior are due to a change in the adsorption coefficient of radium between fresh and salt water and to a change in the average particle concentration between terrestrial and ocean waters (Moore, 1992). Once the particle-enriched river water meets the seawater in the estuary, ^{226}Ra will be desorbed from the particles which results in the increasing of ^{226}Ra in the estuary mixing zone (Elsinger and Moore, 1984; Key et al., 1985; Li et al., 1977; Li and Chan, 1979; Moore and Scott, 1986).

^{226}Ra activities of surface water from several large river estuaries in the world are listed in the Table 3. ^{226}Ra activities show a big variation among the estuaries, but in all cases, ^{226}Ra activities reach the maximum value in the estuary mixing zone. The salinity corresponding to the highest ^{226}Ra activity varies from 7 to 21 (Table 3). Elsinger and Moore (1984) showed ^{226}Ra specific activity ranging from 1.57 to 4.47 Bq/m^3 in the Changjiang River estuary, with the highest value (4.47 Bq/m^3) occurring at a salinity of 9 (Table 3). Zhang (2007) obtained similar results in this estuary. His results showed the ^{226}Ra specific activity ranged from 1.50 to 5.54 Bq/m^3, and the salinity of the sample with highest value (5.54 Bq/m^3) was 11.5 (Table 3). Table 3 also shows that the ^{226}Ra specific activity of the Changjiang River estuary mixing zone was similar to that of the Amazon estuary (Key et al., 1985), but was lower than those of the Mississippi estuary (Moore and Scott, 1986) and Ganges-Brahmaputra estuary (Carroll et al., 1993).

3.2 ^{226}Ra distribution of the surface seawater in the cruise leg from the Changjiang River estuary to 40°S (subtropical front)

From the Hangzhou Bay southward until approaching 40°S, the ^{226}Ra specific activity decreased abruptly and then remained at about 1.00 Bq/m^3 (Fig.2). In these sea areas, the ^{226}Ra specific activities ranged from 0.85 to 1.38 Bq/m^3, with a mean value of 1.07 Bq/m^3 (n=19, SD=0.14).

Many studies on the ^{226}Ra distribution had been conducted in these sea areas. These results clearly showed a ^{226}Ra spatiotemporal variation (Table 4, and as shown by the section from the South China Sea-Indonesia sea area to the Indian Ocean in Fig.3). Six stations had extremely high values (>1.8 Bq/m^3), four of which were located in the Strait of Malacca (stations 13, 14 and 15 of Nozaki and Yamamoto, 2001; station 55 of Okubo et al., 1979), one was located in the west coast of Kalimantan Island (station 54 of Okubo et al., 1979) and one was located in the Bay of Bengal (GEOSECS station 446, Ostlund et al., 1987). These results may imply spatial or/and inter-annual variation of ^{226}Ra in these sea areas, or be the result of different ^{226}Ra measurement methods used by various laboratories. However, our results show the ^{226}Ra specific activities of the surface seawater along this leg are relatively uniform, with a specific activity similar to that of the open ocean (Fig.3). To some extent this is contrary to expectation, because the marine settings along this leg differ greatly.

Table 2 Specific activity of ^{226}Ra in the surface seawater of Prydz Bay and its adjacent sea area

Cruise	Station	Latitude	Longitude	Temperature (°C)	Salinity	Depth (m)	^{226}Ra (Bq/m^3)
CHINARE -19	I-5	65°59′S	67°59′E	-0.334	33.716	2 700	2.26±0.03
	I-7	66°46′S	68°00′E	-0.484	33.110	2 307	2.46±0.03
	I-9	67°00′S	68°02′E	0.165	33.275	1 568	2.26±0.03
	I-11	67°30′S	68°03′E	0.613	34.093	260	2.22±0.03
	I-12	67°40′S	68°01′E	0.077	34.172	484	2.34±0.02
	II-4	65°00′S	70°30′E	1.288	33.559	3 200	2.60±0.04
	II-5	66°01′S	70°29′E	0.943	33.572	2 300	2.96±0.04
	II-7	66°40′S	70°30′E	0.899	33.499	1 869	2.37±0.04
	II-10	67°10′S	70° 40′E	0.496	32.954	295	2.57±0.05
	II-14	68°27′S	70°31′E	1.445	33.817	860	2.56±0.04
	III-8	65°00′S	73°00′E	1.011	33.667	3 000	2.70±0.05
	III-10	66°00′S	73°01′E	1.008	33.623	2 300	2.26±0.05
	III-13(0 m)	66°40′S	73°08′E	1.498	33.641	1 067	2.13±0.04
	III-13(10 m)	66°40′S	73°08′E	0.867	33.661	1 067	2.60±0.04
	III-13(20 m)	66°40′S	73°08′E	0.604	33.688	1 067	2.57±0.04
	III-13(30 m)	66°40′S	73°08′E	-0.151	33.840	1 067	2.26±0.05
	III-15	67°00′S	73°01′E	1.163	33.652	500	2.14±0.04
	III-16	67°32′S	73°01′E	1.055	33.583	587	2.11±0.04
	III-19	68°30′S	72 59′E	0.914	34.106	647	1.92±0.06
	III-20	68°41′S	73°00′E	1.313	34.069	703	2.31±0.05
CHINARE -13	2	69°00′S	75°20′E	n.d.	n.d.	740	2.55±0.06
	3	68°32′S	75°30′E	n.d.	n.d.	650	1.86±0.04
	4	68°01′S	75°27′E	-0.540	33.725	500	2.26±0.04
	5	67°43′S	73°10′E	-0.365	34.034	600	2.09±0.04
	6	67°01′S	73°48′E	-0.571	32.560	450	2.35±0.04
	7	66°22′S	74°08′E	-0.952	32.651	1 000	1.84±0.04
	8	65°29′S	74°03′E	n.d.	n.d.	2 950	2.10±0.04
	9	65°01′S	70°30′E	0.886	33.761	3 200	1.74±0.04
	10	66°01′S	70°40′E	0.201	33.199	3 650	2.18±0.04
	11	68°30′S	72°59′E	0.876	34.033	570	1.84±0.04
	12	68°14′S	71°13′E	n.d.	n.d.	n.d.	2.07±0.05
	13	69°10′S	74°30′E	2.118	34.131	810	2.37±0.04
	14	68°50′S	76°44′E	1.870	34.150	760	2.20±0.04
	15	65°10′S	77°20′E	n.d.	n.d.	n.d.	2.53±0.04

Note: n.d. means no data.

Both the South China Sea and the Java Sea are intensively influenced by the northeast monsoon in the winter and the southwest monsoon in the summer. In the winter, the northeast wind pushes the cooler Chinese coastal waters southward through the Taiwan Straits and into the South China Sea. A portion of this water departs the South China Sea southward into the Java Sea via the Karimata Straits, while other parts turn back northward at the eastern South China Sea, along the coast (Fig.1) (Morton and Blackmore, 2001). The sample stations of this leg were all located in the southward flow area (Fig.1). The strong and fast monsoon induced southward surface flow could overwhelm the local signal of ^{226}Ra, which perhaps leads to the relative uniform feature of ^{226}Ra in these sea areas. These waters ultimately flow into the Indian Ocean by the Indonesian Throughflow, which has long been a focus of research interest and is considered as one of the choke points of the global circulation system.

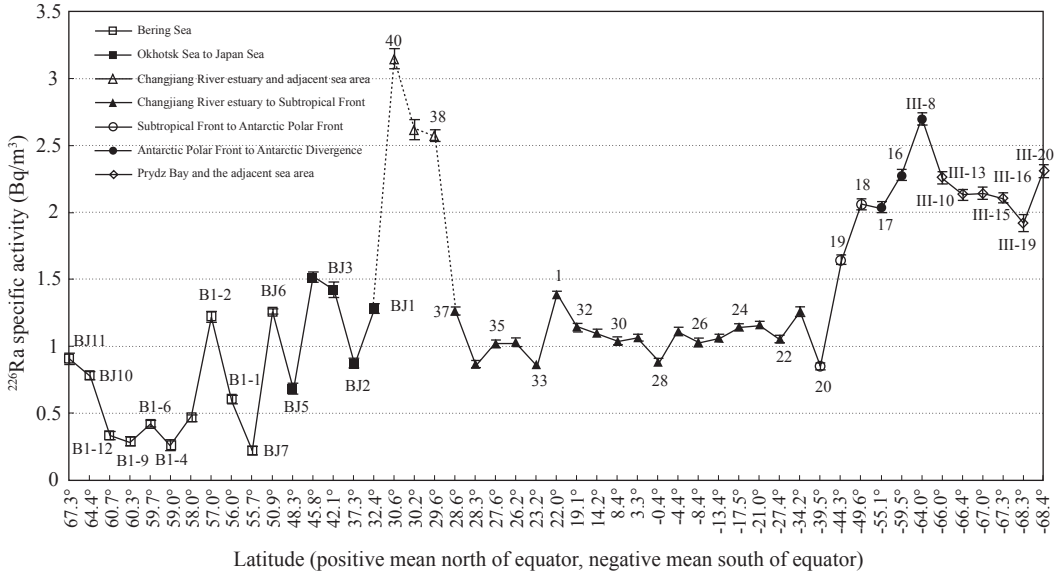

Fig.2 Meridional distribution of ^{226}Ra in the surface seawater from the Bering Sea to Prydz Bay, Antarctica

The Bering Sea- Okhotsk Sea- Japan Sea cited from Xing et al. (2003, 2006).

Table 3 ^{226}Ra specific activity (Bq/m^3) in the surface seawater of the several world large river estuaries

River and sampling time		River water	Mixing zone	Sea water	Reference
Chao Phraya	Jul. 1996	2.28(0.1)*	3.78(6.7)	3.52(21.0)	Nozaki et al., 2001
	Nov. 1996	2.73(0.1)	4.33(8.9)	3.08(23.5)	
Hudson (Oct. 1976)		0.2~0.4(<0.2)	1.42(18.3)	1.38(36.049)	Li and Chan, 1979
Mississippi (Mar. 1983)		2.50(0.11)	5.03(9.51)	1.82(33.60)	Moore and Scott, 1986
Amazon (Dec. 1982)		0.83(0.043)	3.62(21.5)	1.23(36.4)	Key et al., 1985
Delaware		0.57(0.0)	4.28(15.5)	3.12(33.6)	Elsinger and Moore, 1984
Pee Dee (Oct. 1981)		0.88(0.0)	2.62(15.0)	1.38(32.0)	
Yangtze (Changjiang) River		1.57(0.0)	4.47(9.0)	2.28(32.4)	
Changjiang (Oct. 2006)		1.61(0.0)	5.54(11.5)	1.50(33.8)	Zhang, 2007
Bega (Nov. 1991)		0.63(0.1)	3.0(20.0)	1.3(35.8)	Hancock and Murray, 1986
Tagus (Dec. 1989)		0.75(<0.278)	3.85(20.534)	1.20(36.000)	Carvalho, 1997
Ganges-Brahmaputra	Shahbazpur	0.85(0.0)	6.48(10.7)	2.07(31.9)	Carroll et al., 1993
	Haringata	3.75(1.9)	6.15(9.1)	4.77(23.5)	

* Number in parentheses is the salinity of the water with highest ^{226}Ra activity

Most of the Indonesian Throughflow studies have only paid attention to the Indonesian Seas east of Borneo. In fact, the southward-flowing water of the South China Sea also plays an important role (Schott and McCreary, 2001).

The Leeuwin Current is a perennial southward current along the West Australia coast; it is the only poleward-flowing and non-upwelling eastern boundary current globally (Wait et al., 2007). The relationship between the Indonesian Throughflow and Leeuwin Current is still unclear. Some researchers have thought that the South China Sea waters flows into Indian Ocean by the Indonesian Throughflow, and a portion of the Indonesian Throughflow flows southward, forming one source of the Leeuwin Current (Domingues et al., 2007; Schott and McCreary, 2001). The ^{226}Ra distribution feature of this study agrees with this concept.

3.3 ^{226}Ra distribution of surface seawater in the leg from 40°S to Antarctic coastal waters

From 40°S southwards, the ^{226}Ra specific activity of the surface seawater increased intensively (Fig.2), from 0.85 Bq/m^3 at Station 20 to 2.70 Bq/m^3 at Station III-8 (the highest value of this leg), then decreased moderately. Towards the onshore Antarctic,

Table 4 Comparison of ^{226}Ra activities in the surface seawater of some sea areas

Sea area	Sampling time	Mean value of ^{226}Ra (Bq/m^3)	Reference
NE South China Sea	Mar. 1992	1.24 (n=36; SD=0.15)	Xie et al., 1995
	Aug. to Sept. 1994	0.89 (n=17; SD=0.14)	Huang et al., 1997
Southern South China Sea	Sep. to Oct. 1994	1.11 (n=29; SD=0.19)	Huang et al., 1996
	Nov. to Dec. 1993	1.14 (n=29; SD=0.19)	Xie et al., 1996
The South China Sea	Feb. 22 to Feb. 24, 1990	1.31 (n=4, SD=0.04)	Nozaki et al., 1998
The East China Sea (South of Changjiang River)	May to Jun. 1987	1.99 (n=10, SD=0.32)	Nozaki et al., 1991
Leg of South China Sea - Indonesia Sea area - East Indian Ocean	Jan. to Feb., 1997	1.24 (n=16, SD=0.15)	Nozaki and Yamamoto, 2001
	Jan. 13 to Apr. 15, 1976	1.43 (n=12, SD=0.23)	Okubo et al., 1979
	Nov. 1996 to Apr. 1997 and Nov. 1997 to Apr. 1998	0.64 (n=6; SD=0.06)	Wu et al., 2001
	Nov. 1996 to Apr. 1997	1.07 (n=19, SD=0.14)	This study

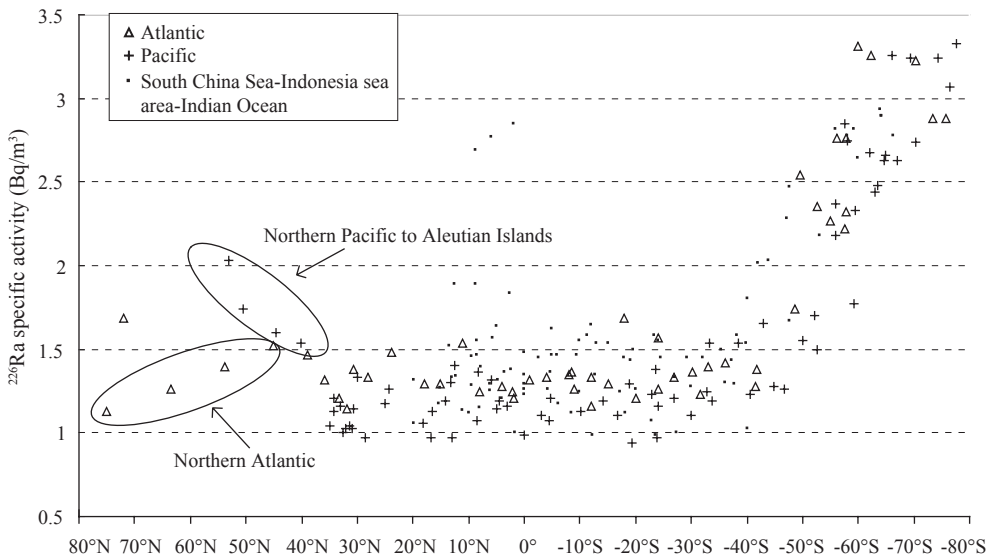

Fig.3 Meridional distribution of ^{226}Ra in the ocean surface seawater

Data cited from: Ku et al., 1970; Chung, 1974; Okubo et al., 1979; Chung and Applequist, 1980; Ostlund et al., 1987; Nozaki et al., 1998; Nozaki and Yamamoto, 2001; Foster et al., 2004.

it again increased by about 0.39 Bq/m^3. Fig.2 clearly shows the feature of increasing ^{226}Ra in the Southern Ocean surface water. Fig.3 indicates that this is a general feature of the Southern Ocean. Ku et al. (1970) first found this feature at a Southern Ocean section south of Australia. They found the ^{226}Ra specific activities of the Southern Ocean deep water were between those of northwest Atlantic and northwest Pacific deep water. However, for the surface water, ^{226}Ra specific activities north of Antarctic Polar Front were similar to those of the northwest Atlantic and northwest Pacific, while south of the Antarctic Polar Front, the ^{226}Ra specific activities were about twice those of the northwest Atlantic and northwest Pacific. Therefore, north of Antarctic Polar Front, the ^{226}Ra specific activity increased with the increasing water depth, while south of Antarctic Polar Front, it had little change with the water depth. This result showed that ^{226}Ra can be used to trace the upwelling of the Circumpolar Deep Water. Latterly, other researchers also observed this phenomenon in other areas of the Southern Ocean (Broecker et al., 1976; Chung, 1974, 1981, 1987; Chung and Craig, 1980; Ku and Lin, 1976). This ^{226}Ra distribution is controlled mainly by the hydrological features of the Southern Ocean.

The continuous eastward-flowing Antarctic Circumpolar Current (ACC) is the main feature of the Southern Ocean. Several main fronts inside the ACC result in large meridional gradients for a lot of oceanographic parameters (Deacon, 1933). From north to south, the first front is the Subtropical Front (STF), or Subtropical Convergence, which is the northern boundary of the ACC, and separates the warm, salty and low ^{226}Ra subtropical water from the Southern Ocean surface water (with high ^{226}Ra). The Subtropical Front is usually distributed along 40°S (He et al., 2003, 2006; Orsi et al., 1995; Yuan et al., 2004), but in the southeast Pacific, it moves northward to 30°S (Orsi et al., 1995). The coordinates of Station 20 (39°46′S, 108°31′E) suggests that it was located in the Subtropical Front. Fig.2 and Table 1 show that from Station 20 southwards, the ^{226}Ra specific activity begins to increase, which agrees with this conclusion. Fig.3 also shows that in the southeast Pacific surface water, the place where ^{226}Ra began increasing moved northward to 30°S, similar to the Subtropical Front (Chung and Craig, 1980; Ku et al., 1980).

The second front is the Antarctic Polar Front, or Antarctic Convergence, which marks the location where the Antarctic surface waters move northwards and sink below the subantarctic water (Deacon, 1933). In the Pacific Ocean, the Antarctic Polar Front is distributed along 65°–60°S, while in the Indian Ocean and the Atlantic Ocean, it is distributed along 50°–55°S (Dong et al., 2006; Kostianoy et al., 2004; Moore et al., 1999; Orsi et al., 1995). Near the sampling section of this study, most studies have shown the Antarctic Polar Front to be located near 50°S (Dong et al., 2006; Kostianoy et al., 2004; Moore et al., 1999; Yuan et al., 2004). In exception, two studies reported that the Antarctic Polar Front was located about 54°S (Gao et al., 2003; He et al., 2006). South of the Antarctic Polar Front, the Circumpolar Deep Water upwells strongly (Deacon, 1933). The most intensive upwelling area is the Antarctic Divergence (AD), which is located between the eastward flowing Antarctic Circumpolar Current and the westward flowing Antarctic coastal Current. Physical oceanography data have shown that the Antarctic Divergence was located between 63°–65°S out of Prydz Bay (He et al., 2003; Nunes Vaz and Lennon, 1996; Park et al., 1998; Smith et al., 1984). The coordinates of Station 18 (49°57′S, 98°02′E) and Station III-8 (65°00′S, 73°00′E) of this study suggest they were located in the Antarctic Polar Front and Antarctic Divergence respectively. The intensive upwelling of the deep water (which has a high ^{226}Ra) leads to the highest ^{226}Ra specific activity for station III-8; mixing of the Antarctic surface waters (high ^{226}Ra) with the subantarctic water (relatively low ^{226}Ra) leads to the moderate ^{226}Ra specific activity for Station 18 (Fig.2). ^{226}Ra specific activity showed a moderate decrease to the south of station III-8; this was the result of the upwelling Circumpolar Deep Water mixing with Prydz Bay surface water. Station III-20 (68°40.6′S, 73°00′E) was the southernmost station of this study. Its ^{226}Ra specific activity increased slightly (0.39 Bq/m^3), probably due to the influence of the continental ^{226}Ra. Studies have shown there to be a positive relationship between ^{226}Ra and H_4SiO_4 (Chung, 1980; Ku et al., 1980). The steep increase of H_4SiO_4 concentration south of the Antarctic Polar Front is a common phenomenon also (Sarmiento and Gruber, 2006).

3.4 ^{226}Ra distribution in the surface seawater of Prydz Bay and its adjacent sea area

Prydz Bay is the third largest bay of the Antarctic, only being smaller than the Weddell and Ross Seas. Its water depth is about 500 to 600 m. The water depth of the inner bay is greater (800 m), deepest (1 085 m) outside the Amery ice shelf (Nunes Vaz and Lennon, 1996). Prydz Bay has been extensively studied, especially its physical oceanography (Dong et al., 2004; Middleton and Humphries, 1989; Nunes Vaz and Lennon, 1996; Pu and Dong, 2003; Smith et al., 1984).

The ^{226}Ra specific activities of the surface seawater of this sea area ranged from 1.74 to 2.96 Bq/m^3, with a mean value of 2.26 Bq/m^3 (n=31，SD=0.28) (Table 2). The ^{226}Ra specific activity was higher at the outer side of the bay and lower in the center of the bay (Fig.4). Yin et al. (2004) reported a similar distribution trend of surface seawater ^{226}Ra in Prydz Bay, although their values were lower than this study.

As Fig.4 shows, ^{226}Ra specific activity was higher in the northern part of the bay. This is possibly due to the northern part of the bay being close to the Antarctic Divergence and under the strong influence of the upwelling Circumpolar Deep Water. Physical oceanography results have indicated that Circumpolar Deep Water might upwell to Prydz Bay near 73°E (Chinese Arctic and Antarctic Administration, 1998; Dong et al., 2004). The water is shallow near the shore and the Fram Bank (Fig.4), so the surface water of these areas can be influenced easily by continental detritus or the ^{226}Ra of marine sediment pore water.

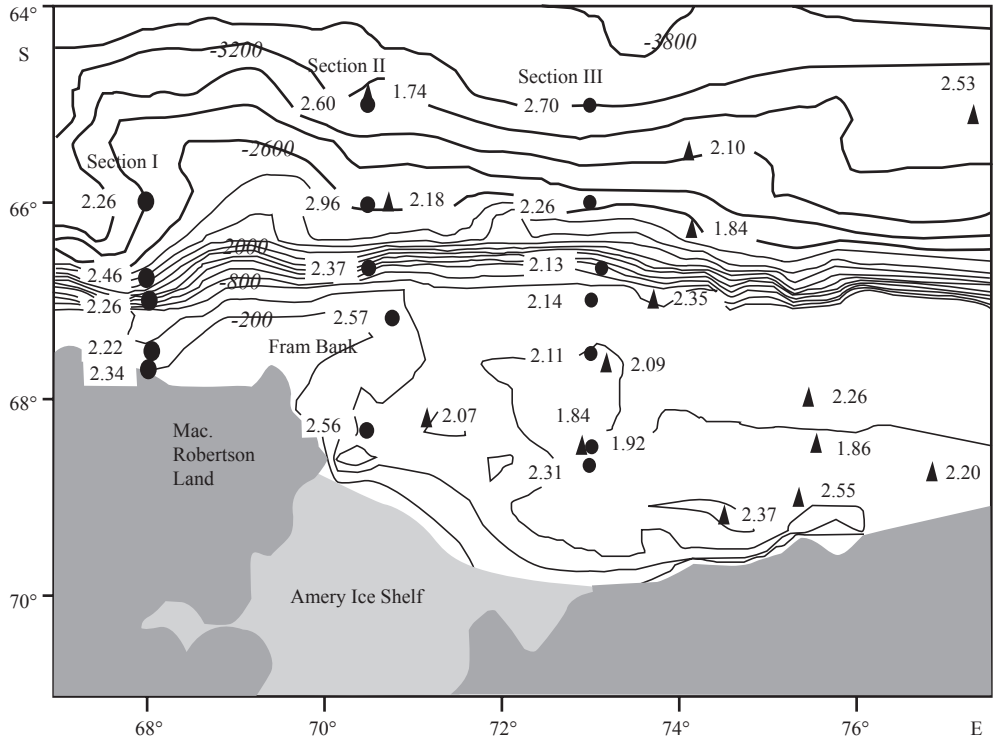

Fig.4 The distribution of ^{226}Ra (Bq/m^3) in the surface seawater of Prydz Bay and its adjacent sea area

▲, ● represent the sampling stations of the 13th and the 19th CHINARE respectively, the numbers near them represent their ^{226}Ra specific activity; italic numbers denote mean water depths (m).

Earlier physical oceanography studies have demonstrated a clockwise cyclonic gyre in Prydz Bay (Middleton and Humphries, 1989; Nunes Vaz and Lennon, 1996; Smith et al., 1984). The water flows into the bay from the eastern coast and flows westward along the coast. At Fram Bank, a part of the water still flows westwards; the rest flows northwards and joins the eastward flowing circumpolar current, forming the clockwise cyclonic gyre (Fig.4). The ^{226}Ra distribution of Prydz Bay surface water (i.e. the higher ^{226}Ra in the outer side of the bay and the lower ^{226}Ra in the center of the bay) agrees with this cyclonic gyre characteristic.

3.5 ^{226}Ra distribution in the surface seawater from the Bering Sea to the Japan Sea

Xing et al. (2003) collected 20 surface seawater ^{226}Ra samples in the Bering Sea. The ^{226}Ra specific activities ranged from 0.25 to 1.26 Bq/m^3, with a mean value of 0.71 Bq/m^3 (n=20, SD=0.33). On the meridian, the section from station B1-1 to station B1-12 had more samples than other sections; therefore the data from this section (Table 5) were used in Fig.2 of this study. Station BJ11 and BJ10 were respectively located at the north and south sides of the Bering Strait (Fig.1), where the water is shallow. Thus, the ^{226}Ra specific activity of those two stations was relatively higher. Stations B1-1 to B1-12 and BJ7 were located at the west side of the Aleutian basin; the water is deeper than 3 000 m for most of the stations (Table 5). With the exception of Station B1-2, all other stations had relatively low ^{226}Ra values (0.22–0.60 Bq/m^3), reflecting the low ^{226}Ra specific activity feature of the southwest Bering Sea. The higher value of the Station B1-2 was possibly due to a measurement problem. Apart from water depth, the dilution of sea ice melt water is another important factor resulting in the low ^{226}Ra. As shown in Table 5, all these samples have lower salinity. Glover and Reeburgh (1987) found the surface seawater ^{226}Ra specific activity was between 0.6 and 1.6 Bq/m^3 along an offshore section in the southeast Bering Sea (water depth range from 50 to 200 m). Considering the factor of water depth, their results were similar to those of this study. However, near the Aleutian Islands, other studies have shown a clear ^{226}Ra specific activity increase (Chung and Craig, 1980; Nozaki et al., 1990) (Fig.3), probably due to the influence of the north Pacific surface water. The high ^{226}Ra specific activity at Station BJ6 may be result from the same influence.

Station BJ5, located outside of Okhotsk Sea, had a ^{226}Ra specific activity value of 0.68 Bq/m^3. Okhotsk Sea has a long frozen period; the sea ice there

Table 5 ^{226}Ra specific activity of surface seawater sampled in the cruise from the Japan Sea to the Bering Sea (Xing et al., 2003, 2006)

Station	Latitude	Longitude	Salinity	Depth (m)	^{226}Ra (Bq/m^3)
BJ11	67°18.7′N	169°49.5′W	31.852	47	0.91±0.04
BJ10	64°21.8′N	166°59.6′W	26.987	n.d.	0.78±0.03
B1-12	60°39.7′N	178°14.2′W	32.168	165	0.33±0.03
B1-9	60°15.2′N	179°25.8′W	32.665	840	0.29±0.03
B1-6	59°39.6′N	179°19.7′E	32.730	3 200	0.42±0.03
B1-4	58°59.4′N	177°55.4′E	32.848	3 720	0.26±0.04
B1-3	58°0.2′N	176°9.4′E	32.968	3 780	0.46±0.02
B1-2	56°59.8′N	174°30.5′E	33.011	3 650	1.22±0.04
B1-1	55°59.8′N	173°21.1′E	32.970	3 850	0.60±0.03
BJ7	55°39.9′N	164°20.4′E	32.673	n.d.	0.22±0.02
BJ6	50°52.1′N	157°51.7′E	32.468	n.d.	1.26±0.04
BJ5	48°15.3′N	149°41.9′E	32.500	n.d.	0.68±0.04
BJ4	45°48.1′N	142°56.0′E	33.493	n.d.	1.51±0.04
BJ3	42°02.9′N	136°19.8′E	33.842	n.d.	1.42±0.05
BJ2	37°19.4′N	131°34.2′E	34.058	n.d.	0.87±0.04
BJ1	32°24.8′N	126°41.3′E	31.586	n.d.	1.28±0.04

Note: n.d. means no data.

can melt completely from Jul. to Oct. each year (Sakamoto et al., 2005). The sampling time of this study was within the ice free period, so both the salinity and the ^{226}Ra specific activity of the sample were low.

The stations from BJ2 to BJ3 were located in the Japan Sea, and stations BJ1 and BJ4 were respectively located in the southern and northern straits of the Japan Sea. The ^{226}Ra specific activity of these samples ranged from 0.87 to 1.51 Bq/m^3, with a mean value of 1.17 (n=4, SD=0.33) (Table 5). Few ^{226}Ra data have been reported for the Japan Sea. Harada and Tsunogai (1986) reported that the surface seawater ^{226}Ra specific activity of the southern Japan Sea ranged from 1.07 to 1.27 Bq/m^3 with a mean value of 1.18 Bq/m^3 (n=8, SD=0.06). This result agrees with our study. Okubo (1980) reported ^{226}Ra specific activity of 3 surface seawater samples of the Japan Sea to be between 1.26 and 1.36 Bq/m^3, slightly higher than in our study.

3.6 Comparison of ^{226}Ra distribution feature in high latitude surface seawater between the southern and northern hemisphere

The distribution features of ^{226}Ra in high latitude surface seawater of the Atlantic, Pacific and Southern Ocean are different, although they are all located in high latitudes, and all are affected by glacier and sea ice. The distribution feature of ^{226}Ra in high latitude surface seawater and its controlling mechanism are discussed in the following.

As show in Figs.2 and 3, the ^{226}Ra specific activities are relatively uniform in the middle and low latitudes sea areas of each ocean. However, at high latitudes, it is different among these oceans. The ^{226}Ra specific activity of surface water increases with latitude both in the Southern Ocean south of 40°S, and from the northern Pacific to the Aleutian Islands, though the extent of increase in the northern Pacific is less than that of the Southern Ocean (Nozaki et al., 1990; Ostlund et al., 1987). In contrast, the ^{226}Ra specific activities of surface water in the northern Atlantic decreases with the increasing latitude, except at station 16 (based on GEOSECS data) (Ostlund et al., 1987). This large scale distribution feature of ^{226}Ra is possibly controlled by the global ocean thermohaline circulation (Broecker and Peng, 1982; Broecker, 1991).

Because the deep water has high ^{226}Ra specific activity, the upwelling of the deep water can lead to the high ^{226}Ra specific activity in the Southern Ocean and the northern Pacific surface water. In the north Atlantic, there is no upwelling of the deep water, and the dilution from melting of sea-ice is greater with the increasing latitude. Therefore the ^{226}Ra specific activity of the northern Atlantic surface water decreases with the increasing latitude. This is

consistent with the distribution of nutrient elements concentration in the world ocean surface water. The concentration of nutrient elements is high for both Southern Ocean and north Pacific surface water, but low for the northern Atlantic surface water (Sarmiento and Gruber, 2006).

4 CONCLUSION

This paper investigated the surface water ^{226}Ra of a transection along the eastern Eurasian continent coastal waters to Prydz Bay, Antarctica. The transection spans a large distance and includes several different marine environments. Our results show the following: 1) The ^{226}Ra specific activity of the Changjiang River estuary mixing zone surface water was the highest value of the study (3.15 Bq/m^3), due to the mixing of river water with the seawater and desorption of ^{226}Ra from the suspended riverine particles; 2) From the Changjiang River estuary to 40°S, the mean value of ^{226}Ra specific activity was 1.07 Bq/m^3 (n=19, SD=0.14); it was relatively uniform even though it spanned over 70 latitude degrees and traversed several different marine environments. This is possibly the result of the strong northeastern monsoon, which overwhelmed the local signal of ^{226}Ra; 3) Surface seawater ^{226}Ra specific activity increased sharply southwards from 40°S. This agrees with the published data, and was probably the result of the deep water upwelling; 4) The ^{226}Ra distribution in surface water in Prydz Bay was higher around the bay, but lower in the center of the bay; this is consistent with the topography and hydrological features of the Prydz Bay; 5) The large scale ^{226}Ra distribution of world oceanic surface seawater is possibly controlled by the ocean thermohaline circulation.

5 ACKNOWLEDGMENT

The scientists and the crew of R/V *Xue Long* provided a lot of help during the sample collection. Senior Engineer Yutian JIAO provided the hydrological data; Dr. KUMAR M. D. helped to obtain the GEOSECS ^{226}Ra data of eastern Indian Ocean; Prof. Gangshan LIU and Senior Engineer Yusheng QIU provided a lot of support and help in the activity measurement. Drs. Rutgers v. d. Loeff M., Moore W. S. and the three anonymous reviewers give insightful comments on this manuscript. Dr. Hu LI helped to improve the English. We heartily thank all of them.

References

Broecker W S, Godard J, Sarmiento J L. 1976. The distribution of ^{226}Ra in the Atlantic Ocean. *Earth Planet. Sci. Lett.*, **32**: 220-235.

Broecker W S, Peng T H. 1982. Tracers in the Sea. Eldigio Press, Palisades, New York. p.34-200.

Broecker W S. 1991. The Great Ocean conveyor. *Oceanography*, **4**: 79-89.

Carroll J, Falkner K K, Brown E T, Moore W S. 1993. The role of the Ganges-Brahmaputra mixing zone in supplying barium and ^{226}Ra to the Bay of Bengal. *Geochim. Cosmochim. Acta*, **57**: 2 981-2 990.

Carvalho F P. 1997. Distribution, cycling and mean residence time of ^{226}Ra, ^{210}Pb and ^{210}Po in the Tagus estuary. *Sci. Total Environ.*, **196**: 151-161.

Chinese Arctic and Antarctic Administration. 1998. Results and Progress of Chinese Antarctic Expedition. China Ocean Press, Beijing, China. p.17-33. (in Chinese)

Chung Y C. 1974. Radium-226 and Ra-Ba relationships in Antarctic and Pacific waters. *Earth Planet. Sci. Lett.*, **23**: 125-135.

Chung Y C, Craig H. 1980. ^{226}Ra in the Pacific Ocean. *Earth Planet. Sci. Lett.*, **49**: 267-292.

Chung Y. 1980. Radium-barium-silica correlation and a two-dimensional radium model for the world ocean. *Earth Planet. Sci. Lett.*, **49**: 309-318.

Chung Y, Applequist M D. 1980. ^{226}Ra and ^{210}Pb in the Weddell Sea. *Earth Planet. Sci. Lett.*, **49**: 401-410.

Chung Y C. 1981. ^{210}Pb and ^{226}Ra distributions in the Circumpolar waters. *Earth Planet. Sci. Lett.*, **55**: 205-216.

Chung Y C. 1987. ^{226}Ra in the western Indian Ocean. *Earth Planet. Sci. Lett.*, **85**: 11-27.

Deacon G E R. 1933. A general account of the hydrology of the South Atlantic Ocean. *Discovery Reports*, **7**: 171-238.

Domingues C M, Maltrud M E, Wijffels S E. 2007. Simulated Lagrangian pathways between the Leeuwin Current System and the upper-ocean circulation of the southeast Indian Ocean. *Deep-Sea Res. II*, **54**: 797-817.

Dong Z Q, Pu S Z, Hu X M, Yu F, He Z G. 2004. Water mass study of Prydz Bay and adjacent sea area. *In*: Chen L Q ed. The Response and Feed Back of Antarctic Area to the Global Climate Change. China Ocean Press, Beijing, China. p.13-25. (in Chinese)

Dong S F, Sprintall J, Gille S T. 2006. Location of the Antarctic Polar Front from AMSR-E satellite sea surface temperature measurements. *J. Phys. Oceanogr.*, **36**: 2 075-2 089.

Elsinger R J, Moore W S. 1984. Ra-228 and Ra-226 in the mixing zones of the Pee Dee River-Winyah Bay, Yangtze River, and Delaware Bay Estuaries. *Estuar. Coast. Shelf Sci.*, **18**: 601- 613.

Foster D A, Staubwasser M, Henderson G M. 2004. ^{226}Ra and Ba concentrations in the Ross Sea measured with multicollector ICP mass spectrometry. *Mar. Chem.*, **87**: 59-71.

Gao G P, Han S Z, Dong Z Q, Yang S Y. 2003. Structure and variability of fronts in the South Indian Ocean along sections from Zhongshan Station to Fremantle. *Acta Oceanol. Sin.*, **25**: 9-19. (in Chinese with English abstract)

Glover D M, Reeburgh W S. 1987. Rn-222 and Ra-226 in southeastern Bering Sea shelf waters and sediment. *Cont*. *Shelf Res*., **7**: 433-456.

Hancock G J, Murray A S. 1996. Source and distribution of dissolved radium in the Bega River estuary, Southeastern Australia. *Earth Planet*. *Sci*. *Lett*., **138**: 145-155.

Harada K, Tsunogai L. 1986. ^{226}Ra in the Japan Sea and the residence time of the Japan Sea water. *Earth Planet*. *Sci*. *Lett*., **77**: 236-244.

He Z G, Dong Z Q, Hu J Y. 2003. Upper ocean hydrographic properties of southeast Indian Ocean in austral summer, 2003. *Chinese J*. *Polar Res*., **15**: 195-206. (in Chinese with English abstract)

He Z G, Dong Z Q, Yuan X J. 2006. Fronts and strong currents of the upper southeast Indian Ocean. *Acta Oceanol*. *Sin*., **25**: 1-24.

Huang Y P, Chen X B, Jiang D S, Xie Y Z, Qiu Y S, Chen F Z, Cai P H. 1996. Distribution and variation of ^{226}Ra in the Nansha sea area during 1994 cruise. *In*: Huang Y P ed. Isotope Marine Chemistry of Nansha Islands Waters. China Ocean Press, Beijing, China. p.79-88. (in Chinese with English abstract)

Huang Y P, Jiang D S, Xu M Q, Chen M, Qiu Y S. 1997. The distribution of ^{226}Ra in the surface water of the northeastern South China Sea. *Tropic Oceanogr*., **16**: 75-81. (in Chinese with English abstract)

Hussain N, Church T M, Kim G. 1999. Use of ^{222}Rn and ^{226}Ra to trace groundwater discharge into the Chesapeake Bay. *Mar*. *Chem*., **65**: 127-134.

Hwang D W, Kim G, Lee Y W, Yang S H. 2005. Estimating submarine inputs of groundwater and nutrients to a coastal bay using radium isotopes. *Mar*. *Chem*., **96**: 61-71.

Inoue M, Tanaka K, Kofuji H, Nakano Y, Komura K. 2007. Seasonal variation in the ^{228}Ra/^{226}Ra ratio of coastal water within the Sea of Japan: Implications for the origin and circulation patterns of the Tsushima Coastal Branch Current. *Mar*. *Chem*., **107**: 559-568.

Key R M, Stallard R F, Moore W S, Sarmiento J L. 1985. Distribution and flux of ^{226}Ra and ^{228}Ra in the Amazon River estuary. *J*. *Geophys*. *Res*., **90**: 6 995-7 004.

Kim G, Ryu J W, Yang H S, Yun S T. 2005. Submarine groundwater discharge (SGD) into the Yellow Sea revealed by ^{228}Ra and ^{226}Ra isotopes: Implications for global silicate fluxes. *Earth Planet*. *Sci*. *Lett*., **237**: 156-166.

Koczy F F. 1958. Natural radium as a tracer in the ocean. *In*: Proceedings of the Second UN International Conference on Peaceful Uses of Atomic Energy. Geneva. Vol. 18, p.351-357.

Kostianoy A G, Ginzburg A I, Frankignoulle M, Delille B. 2004. Fronts in the Southern Indian Ocean as inferred from satellite sea surface temperature data. *J*. *Mar*. *Syst*., **45**: 55-73.

Krest J M, Moore W S, Rama. 1999. ^{226}Ra and ^{228}Ra in the mixing zones of the Mississippi and Atchafalaya Rivers: indicators of groundwater input. *Mar*. *Chem*., **64**: 129-152.

Ku T L, Li Y H, Mathieu G G, Wong H K. 1970. Radium in the Indian-Antarctic Ocean South of Australia. *J*. *Geophys*. *Res*., **75**: 5 286-5 292.

Ku T L, Lin M C. 1976. ^{226}Ra distribution in the Antarctic Ocean. *Earth Planet*. *Sci*. *Lett*., **32**: 236-248.

Ku T L, Huh C A, Chen P S. 1980. Meridional distribution of ^{226}Ra in the eastern Pacific along GEOSECS cruise tracks. *Earth Planet*. *Sci*. *Lett*., **49**: 293-308.

Lee J S, Kim K H, Moon D S. 2005. Radium isotopes in the Ulsan Bay. *J*. *Environ*. *Radioact*., **82**: 129-141.

Li Y H, Mathieu G, Biskaye P, Simpson J H. 1977. The fluxes of ^{226}Ra from estuarine and continental shelf sediments. *Earth Planet*. *Sci*. *Lett*., **37**: 237-241.

Li Y H, Chan L H. 1979. Desorption of Ba and ^{226}Ra from river-borne sediments in the Hudson Estuary. *Earth Planet*. *Sci*. *Lett*., **43**: 343-350.

Li Y P, Chen M, Huang Y P, Cai Y H. 2004. Surface distribution and temporal change of ^{226}Ra and ^{228}Ra in the North Pacific Subtropical Gyre. *J*. *Oceanogr*. *Taiwan Strait*, **23**: 261-267. (in Chinese with English abstract)

Men W, Wei H, Liu G S. 2006. ^{226}Ra and ^{228}Ra in the seawater of the Western Yellow Sea. *J*. *Ocean Univ*. *China* (*Oceanic and Coastal Sea Research*), **15**: 228-234.

Men W. 2008. The study on the oceanography of the Yellow Sea and the East China Sea traced by radium isotopes. Ph.D. thesis, Xiamen University, Xiamen, China. (in Chinese with English abstract)

Middleton J H, Humphries S E. 1989. Thermohaline structure and mixing in the region of Prydz Bay, Antarctica. *Deep Sea Res*., **36**: 1 255-1 266.

Moore D G, Scott M. 1986. Behavior of ^{226}Ra in the Mississippi River mixing zone. *J*. *Geophys*. *Res*., **91**: 14 317-14 329.

Moore J K, Abbott M R, Richman J G. 1999. Location and dynamics of the Antarctic Polar Front from satellite sea surface temperature data. *J*. *Geophys*. *Res*., **104**: 3 059-3 073.

Moore W S, Reid D F. 1973. Extraction of radium from natural waters using manganese-impregnated acrylic fibers. *J*. *Geophys*. *Res*., **78**: 8 880-8 886.

Moore W S. 1992. Radionuclides of the uranium and thorium decay series in the estuary environment. *In*: Ivanovich M et al. eds. Uranium Series Disequilibrium: Applications to Earth, Marine and Environmental Sciences. Clarendon Press, Oxford. p.405.

Moore W S, Astwood H, Lindstrom C. 1995. Radium isotopes in coastal waters on the Amazon shelf. *Geochim*. *Cosmochim*. *Acta*, **59**: 4 285-4 298.

Moore W S. 1996. Large groundwater inputs to coastal waters revealed by ^{226}Ra enrichments. *Nature*, **380**: 612-614.

Moore W S. 2000. Determination coastal mixing rates using radium isotopes. *Continental Shelf Research*, **20**: 1 993-2 007.

Morton B, Blackmore G. 2001. South China Sea. *Mar*. *Pollut*. *Bull*., **42**: 1 236-1 263.

Nozaki Y, Kasemupava V, Tsubota H. 1989. Mean residence time of the shelf water in the East China and the Yellow Seas determined by ^{228}Ra/^{226}Ra measurements. *Geophys*. *Res*. *Lett*., **16**: 1 297-1 300.

Nozaki Y, Kasemsupaya V, Tsubota H. 1990. The distribution of ^{228}Ra and ^{226}Ra in the surface waters of the northern North Pacific. *Geochem*. *J*., **24**: 1-6.

Nozaki Y, Tsubota H, Kasemupava V, Yashima M, Naoko I. 1991. Residence time of surface water and particle-reactive ^{210}Pb and ^{210}Po in the East China and Yellow Seas. *Geochim*. *Cosmochim*. *Acta*, **55**: 1 265-1 272.

Nozaki Y, Dobashi F, Kato Y, Yamamoto Y. 1998. Distribution of Ra isotopes and the ^{210}Pb and ^{210}Po balance in surface seawaters of the mid Northern Hemisphere. *Deep-Sea Res*. *I*, **45**: 1 263-1 284.

Nozaki Y, Yamamoto Y. 2001. Radium 228 based nitrate fluxes in the eastern Indian Ocean and South China Sea and a silicon-induced "alkalinity pump" hypothesis. *Glob*. *Biogeochem*. *Cycle*, **15**: 555-567.

Nozaki Y, Yamamoto Y, Manakaa T, Amakawa H, Snidvongs A. 2001. Dissolved barium and radium isotopes in the Chao Phraya River estuarine mixing zone in Thailand. *Cont*. *Shelf Res*., **21**: 1 435-1 448.

Nunes Vaz R A, Lennon G W. 1996. Physical oceanography of the Prydz Bay region of Antarctic waters. *Deep-Sea Res*. *I*, **43**: 603-641.

Okubo T, Furuyama K, Sakanoue M. 1979. Distribution of ^{228}Ra in surface sea water of the East Indian Ocean. *Geochem*. *J*. **13**: 201-206.

Okubo T. 1980. Radium-228 in the Japan Sea. *J*. *Oceanogr*. *Soc*. *Japan*, **36**: 263-268.

Orsi A H, Whitworth III T, Nowlin Jr W D. 1995. On the meridional extent and fronts of the Antarctic Circumpolar Current. *Deep-Sea Res*. *I*, **42**: 641-673.

Ostlund H G, Craig H, Broecker W S, Spencer D W. 1987. GEOSECS Atlantic, Pacific and Indian Ocean Expeditions, Vol.7, Shorebased data and graphics. National Science Foundation, U.S. Government Printing Office, Washington D.C. Visible also in: http://climotope.earth.ox.ac.uk/research/oceanic_u-series_database/geosecs_226ra_dataset_notes_and_references. (Accessed on 2010-06-06).

Park Y H, Charriaud E, Fieux M. 1998. Thermohaline structure of the Antarctic Surface Water/Winter Water in the Indian sector of the Southern Ocean. *J*. *Mar*. *Syst*., **17**: 5-23.

Pu S Z, Dong Z Q. 2003. Progress in physical oceanographic studies of Prydz Bay and its adjacent oceanic area. *Chinese J*. *Polar Res*., **15**: 53-64. (in Chinese with English abstract)

Sarmiento J L, Gruber N. 2006. Ocean Biogeochemical Dynamics. Princeton University Press. p.270-317.

Schott F A, McCreary Jr J P. 2001. The monsoon circulation of the Indian Ocean. *Progress in Oceanography*, **51**: 1-123.

Sakamoto T, Ikehara M, Aoki K. 2005. Ice-rafted debris (IRD)-based sea-ice expansion events during the past 100 kyrs in the Okhotsk Sea. *Deep-Sea Res*. *II*, **52**: 2 275-2 301.

Shi W Y, Qiu X H, Huang Y P. 1993. Distribution of ^{226}Ra in the Jiulong River estuary. *Acta Oceanol*. *Sin*., **15**: 50-55. (in Chinese)

Smith N R, Dong Z Q, Kerry K R, Wright S. 1984. Water masses and circulation in the region of Prydz Bay, Antarctica. *Deep-Sea Res*., **31**: 1 121-1 147.

Waite A M, Thompson P A, Pesant S, Feng M, Beckley L E, Domingues C M, Gaughan D, Hanson C E, Holl CM, Koslow T, Meuleners M, Montoya J P, Moore T, Muhling B A, Paterson H, Rennie S, Strzelecki J, Twomey L. 2007. The Leeuwin Current and its eddies: An introductory overview. *Deep-Sea Res*. *II*, **54**: 789-796.

Wu S Y, Yin M D, Zeng X Z, Zeng W Y, Shi C T. 2001. Distribution of ^{226}Ra in the surface water of the oceans. *J*. *Tropical Oceanogr*., **20**: 54-59. (in Chinese with English abstract)

Xie Y Z, Huang Y P, Shi W Y, Xu M Q, Qiu Y S, Ruan D J. 1994a. ^{228}Ra and ^{226}Ra in the Jiulong River estuary. *J*. *Oceanogr*. *Taiwan Strait*, **134**: 394-399. (in Chinese with English abstract)

Xie Y Z, Huang Y P, Shi W Y, Qiu Y S. 1994b. Simultaneous concentration and determination of ^{226}Ra, ^{228}Ra in natural water. *J*. *Xiamen Univ*. **33**(suppl.): 86-90. (in Chinese with English abstract)

Xie Y Z, Shi W Y, Huang Y P, Fu Z L, Qiu Y S, Xiao Y, Chen M, Chen F Z. 1995. ^{226}Ra in the NE South China Sea. *In*: Yu X Q ed. Proceedings of Symposium of Marine Sciences in Taiwan Strait and its Adjacent Waters, China Ocean Press, Beijing, China. p.225-231. (in Chinese with English abstract)

Xie Y Z, Huang Y P, Qiu Y S, Chen M, Chen F Z. 1996. Distribution of ^{226}Ra in surface water of the Nansha sea area. *In*: Huang Y P ed. Isotope Marine Chemistry of Nansha Islands Waters, China Ocean Press, Beijing, China. p.63-69. (in Chinese with English abstract)

Xing N, Chen M, Huang Y P, Cai P H, Qiu Y S. 2003. Distribution of ^{226}Ra in the Arctic Ocean and the Bering Sea and its hydrologic implications. *Sci*. *China* (*Series D*), **46**: 516-528.

Xing N, Chen M, Huang Y P, Qiu Y S. 2006. Distribution of surface ^{226}Ra, ^{228}Ra and ^{210}Pb under the way of Chinese First Arctic Expedition. *In*: Huang Y P et al. eds. Treatise on Marine Chemistry. China Ocean Press, Beijing, China. p.191-201. (in Chinese with English abstract)

Yang J H, Chen M, Qiu Y S, Li Y P, Ma Q, Liu E, Zhang R, Huang Y P. 2007. ^{226}Ra evidence for the ecosystem shift over the past 40 years in the North Pacific Subtropical Gyre. *Chinese Sci*. *Bull*., **52**: 832-838.

Yin M D, Zeng W Y, Wu S Y, Zeng X Z, Huo X J. 2004. Distribution of uranium-series isotopes in the Prydz Bay, Antarctica. *Chinese J*. *Polar Res*., **16**: 11-21. (in Chinese with English abstract)

Richardson P L. 2008. On the history of meridional overturning circulation schematic diagrams. *Prog*. *Oceanogr*., **76**: 466-486.

Yuan X J, Martinson D G, Dong Z Q. 2004. Upper ocean thermohaline structure and its temporal variability in the southeast Indian Ocean. *Deep-Sea Res*. *I*, **51**: 333-347.

Zhang L, Liu Z, Zhang J, Hong G H, Park Y, Zhang H F. 2007. Reevaluation of mixing among multiple water masses in the shelf: An example from the East China Sea. *Cont*. *Shelf Res*., **27**: 1 969-1 979.

Zhang L. 2007. Radium isotopes in Changjiang estuary/East China Sea and their application in analysis of mixing among multiple water mass. Ph.D. thesis, East China Normal University, 138p.